Exotic decays of top partners: Mind the search gap

Giacomo Cacciapaglia [a,b], Thomas Flacke [c,*], Myeonghun Park [c,d], Mengchao Zhang [e,c,1]

[a] *Institut de Physique des 2 Infinis (IP2I), CNRS/IN2P3 UMR5822, 69622 Villeurbanne, France*
[b] *Univ Lyon, Université Claude Bernard Lyon 1, 69001 Lyon, France*
[c] *Center for Theoretical Physics of the Universe, Institute for Basic Science (IBS), Daejeon 34126, Republic of Korea*
[d] *Institute of Convergence Fundamental Studies and School of Liberal Arts, Seoultech, 232 Gongneungro, Nowon-gu, Seoul, 01811, Republic of Korea*
[e] *Department of Physics and Siyuan Laboratory, Jinan University, Guangzhou 510632, PR China*

ARTICLE INFO

ABSTRACT

Many standard model extensions, including composite Goldstone Higgs models, predict vector-like fermionic top-partners at the TeV scale. The intensive search programmes by ATLAS and CMS focus on decays into a 3$^{\rm rd}$ generation quark and an electroweak boson (W, Z, h). However, underlying models of partial compositeness contain additional states that give rise to exotic top partner decays. We consider a well-motivated scenario in which a charge-2/3 top-partner decays into a pseudo-scalar, $T \to t\, a$, with $a \to gg$ or $b\bar{b}$ dominating below the $t\bar{t}$ threshold. We show that the constraints on the top partner mass from QCD pair production are substantially weakened, still allowing a top partner mass as light as 400 GeV.

Top parters, i.e. vector-like quarks that couple to the top (and bottom) quarks, are a crucial ingredient in models of composite Goldstone Higgs [1] with top partial compositeness [2]. They are usually expected to have masses between ≈ 1 to several TeV, with the lightest masses preferable if they play the role of regulators of the top loop corrections to the Higgs mass [3]. Following the minimal coset [4], they are expected to decay into a top or bottom, plus a Standard Model (SM) massive boson: for a top partner of charge 2/3, T, the standard decay channels are thus $T \to b\, W^+$, $t\, Z$ and $t\, h$ [5]. Both ATLAS and CMS at the Large Hadron Collider (LHC) have extensive search programmes tailored to search for these states, leading to current bounds in the range $1.30 \div 1.42$ TeV depending on their branching ratios (BRs) [6–15].

Recently there has been raising interest in exploring "exotic" decays into non-SM bosons: they could arise as new pseudo-Nambu-Goldstones in non-minimal cosets [16–19], as additional pseudo-scalars carrying QCD colour charge [17], as Dark Matter candidates [20,21], or they could be a gluon or a photon [22,23] or simply new scalar states [19,24–26]. Exotic decays of a charge 5/3 top partner have been extensively studied in Ref. [27]. While in this work we are interested in composite Higgs models, top part-

ners also arise in other classes of models: extra dimensions (from which modern composite Goldstone Higgs models derive via the principle of holography [28][2]), Little-Higgs models [31] (which can also be thought of as composite, see for instance [32]), and models where vector-like quarks are added "by hand" to the theory, like in supersymmetry [24] and two-Higgs-doublet models [19,25,26]. Thus most of the results presented in this work can be extended to those scenarios.

In this letter we are interested in composite Goldstone Higgs models that feature an "axion-like" pseudo-scalar a arising as a pseudo-Nambu-Goldstone boson from a global $U(1)$ symmetry. In models with an underlying gauge-fermion description [33,34], this state is ubiquitous [35–37] and it can be potentially much lighter than the compositeness scale [36]. In Ref. [17] it has been shown that it can have sizeable couplings to the top partners, in particular allowing decays of the charge-2/3 top partner $T \to t\, a$. The Lagrangian of the pseudo-scalar a is given by

$$\mathcal{L}_a = \frac{1}{2}(\partial_\mu a)(\partial^\mu a) - \frac{1}{2}m_a^2 a^2 + \sum_i \frac{g_i^2 K_i^a}{16\pi^2 f_a} a \mathcal{G}_{\mu\nu}^i \tilde{\mathcal{G}}^{i\mu\nu}$$

$$- \sum_f \frac{iC_f^a m_f}{f_a} a \bar{f} \gamma^5 f, \qquad (0.1)$$

[2] Holographic interpretations of top partners can be found in Refs. [29,30].

where $\mathcal{G}^i$ denote the $SU(3)_c \times SU(2)_L \times U(1)_Y$ field strengths[3] and f denotes SM fermions. The decay constant f_a is related to the composite Higgs decay constant f_h that is expected to lie in the TeV range, and the coupling constants K_i^a and C_f^a are dictated by the quantum numbers of the underlying fermions, and are thus fixed for each underlying model (we refer the reader to Ref. [36] for a comprehensive review and to Ref. [38] for numerical tables of coefficients). While the precise numerical values vary among different models, the branching ratios share the following features: above the $t\bar{t}$ threshold, $m_a > 2m_t$, the dominant decay is into tops, while below the dominant decay is in a pair of gluons, $a \to gg$, with decays into heavy fermions following, $a \to b\bar{b}$, $\tau^+\tau^-$.

The coupling to gluons allows for copious direct production of a at the LHC, and bounds from direct searches have been exhaustively studied in Refs. [36,38,39]. Interestingly, there is a mass window 15 GeV $\lesssim m_a \lesssim 65$ GeV where very weak constraints apply.[4] In the remaining mass range, significant bounds apply on f_a from various channels, which, once converted to bounds on the Higgs decay constant f_h, are often stronger than those from electroweak precision tests. For this reason we will focus in this letter on the low mass range and establish if significant bounds can derive from the production of a via T decays. Are there gaps in the LHC search coverage for these signatures? How low can the bound on the T mass be? Our main goal will be to answer these questions and guide the experimental effort toward a complete coverage of top partner signatures.

1. Phenomenology of a top partner in presence of $T \to t\,a$ decays

As a simplified model, we introduce the top partner T with charge 2/3, with the following Lagrangian [17]

$$
\begin{aligned}
\mathcal{L}_T = \ & \overline{T}\left(i\slashed{D} - m_T\right)T + \left(\kappa_{W,L}^T \frac{g}{\sqrt{2}} \overline{T}\slashed{W}^+ P_L b \right. \\
& + \kappa_{Z,L}^T \frac{g}{2c_W}\overline{T}\slashed{Z}P_L t - \kappa_{h,L}^T \frac{m_T}{v}\overline{T}h P_L t \\
& \left. + i\kappa_{a,L}^T \overline{T}a P_L t + L \leftrightarrow R + \text{h.c.}\right),
\end{aligned}
\tag{1.1}
$$

where $P_{L,R}$ are left- and right-handed projectors, and T denotes the top partner mass eigenstate with mass m_T. The first three interaction terms dictate the partial widths of T decays into $b\,W$, $t\,Z$, and $t\,h$ as often considered in vector-like quark models [41, 42], while the decay into $t\,a$ is the new "exotic" decay we consider. As shown in Ref. [17], in underlying models with top partial compositeness the branching ratio $T \to t\,a$ can be sizeable and even dominate over the "standard" ones. Note that the couplings are always dominantly chiral, i.e. they either involve left-handed t and b, or right-handed ones.

As the pseudo-scalar a has small couplings to SM particles other than the top, it has a minor effect on T production. The top partner T is, therefore, single-produced in $b\,W$ and $t\,Z$ fusion (see Fig. 1, left) or pair-produced via its QCD interaction (see Fig. 1, right), as is commonly considered. The presence of a affects the searches by providing an additional decay channel, $T \to t\,a$, with the signatures depending on the decay modes of a. The cases of decays into $t\bar{t}$ and into a pair of electroweak gauge bosons have been studied in Refs. [18,19,27], showing a good coverage from current searches and prospects for improvements. In this letter we will focus on the more challenging decays $a \to gg$ and $a \to b\bar{b}$,
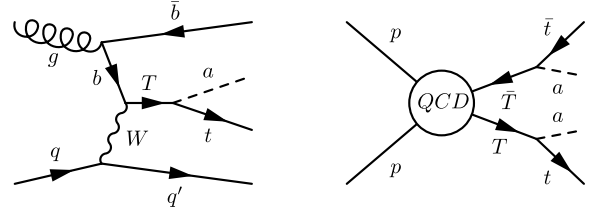

Fig. 1. Example top partner production processes for electroweak single-production (left) and QCD pair production (right).

which dominate at low mass. We should mention that searches targeting $\tau^+\tau^-$ may also be relevant [39] as well as the more suppressed di-muon channel [43,44].

We will focus on pair production due to QCD interactions, which has the benefit of only depending on the mass m_T. To a good approximation, pair production with subsequent decays into $t\,a$, $t\,h$, $t\,Z$, $b\,W$ is characterised by three branching ratios (assuming that there are no additional channels), while the kinematics of the new channel depend on m_a and the dominant decay channel of a. We will assume here that T has a small width so that production and decay can be factorised,[5] and under this approximation it is justifiable to neglect single production which is proportional to the couplings $\kappa_{W/Z/h/a,L/R}^T$ in eq. (1.1). Moreover, we will neglect the effect of the top and bottom polarisation, which only affects the final state kinematics in a minor way.

ATLAS and CMS pursue an active search program for vector-like quarks, with several searches for pair-produced T targeting decays into $T \to t\,h$, $t\,Z$, $b\,W$ extended to the $\sqrt{s} = 13$ TeV data [6–11, 13–15]. Both collaborations provide bounds in benchmarks as well as in "branching ratio triangle" summary plots, assuming BR($T \to t\,h$) + BR($T \to t\,Z$) + BR($T \to b\,W$) = 1. ATLAS provides a combination of its individual searches [12] which established a lower bound on m_T of $1300 \div 1420$ GeV, depending on the T branching ratios, with the strongest bound applying for BR$_{T \to th}$ = 100%. The CMS bounds are comparable, with $m_T > 1370 / 1300 / 1295$ GeV for 100% BR into th / tZ / bW [13–15].[6]

How are these bounds modified in the presence of the $T \to t\,a$ decay? Pair production searches are still mainly based on a cut-and-count method. The number of signal events in a given signal region is

$$
N_s = \mathcal{L}\,\sigma_{T,p}(m_T) \sum_{ij} \epsilon_{ij}(m_T)\,\text{BR}_i\,\text{BR}_j,
\tag{1.2}
$$

where $\mathcal{L}$ is the integrated luminosity used in the search, $\sigma_{T,p}$ is the $pp \to T\overline{T}$ production cross section (which depends on m_T), and $i,j = W, Z, h, a$ label the different decay channels of T. The factor ϵ_{ij} is the signal efficiency for a pair-produced T with one T decaying through decay i with branching BR$_i$ and its charge conjugate through decay j with branching BR$_j$. Fully determining the bound on m_T would require knowledge of all $\epsilon_{ij}(m_T)$ for each search signal region. Typically, the searches are designed in such a way that each signal region targeting a specific final state, $t\,Z$, $t\,h$ or $b\,W$, has very low sensitivity to the others, so that the signatures are picked up exclusively by one search. However, this is not the case for the new channel, which can in principle populate different signal regions. One conservative approach consists in ignoring the new channel and rescale the bound with the reduced BR in the standard channels [24], and a discussion is currently undergoing within the experimental collaborations on ways

---

[3] Note that the $U(1)$ pseudo-scalar is the only state that can couple to both gluons and electroweak gauge bosons in gauge-fermion underlying models.

[4] Contrary to the generic analysis of Ref. [40], decays of the Higgs boson $h \to aa$ and $h \to Za$ pose very weak constraints [39] in these models.

[5] See Ref. [45] for large-width effects in vector-like quark pair production.

[6] The CMS searches are not combined, yet.

to update the triangle summary plots.[7] In this letter we will discuss how the new signature affects the bound in some motivated benchmark points by recasting the relevant searches.

2. Bounds for exclusive decays, $BR(T \to t\,a) = 100\%$, $a \to gg$, $b\bar{b}$

We first focus on exclusive decays in the new channel, and we identify 3 searches that are sensitive to decays $a \to gg$ and $a \to b\bar{b}$. As our main interest is on the low mass region, the final states may be boosted thus leading to merging jets. The three searches we recast are:

- For very light a, the two jets are strongly collimated and a can be mis-identified as a single QCD jet. The final state is, therefore, similar to $t\bar{t}jj$ and we recast the CMS search for "excited tops" at $\sqrt{s} = 13$ TeV [46] to cover this region.
- For larger m_a, the di-jet system becomes resolved and, for hadronically decaying tops, the final state contains many energetic jets. Searches for R-parity violating supersymmetry (RPV SUSY) in hadronic final states can cover the target signature. We thus recast the ATLAS $\sqrt{s} = 8$ TeV search from Ref. [47]. The most recent $\sqrt{s} = 13$ TeV in Ref. [48] applies a much stronger cut on the summed jet-mass, which rejects most of the signal and, therefore, is less sensitive to our final state (see Appendix A.3 for details). Similarly, the CMS $\sqrt{s} = 13$ TeV RPV SUSY search [49] requires a high summed jet-mass and a high H_T cut.
- If m_a is close to the W-Z or Higgs masses, it can be mis-tagged as a hadronically decaying SM boson. Thus, standard top partner searches could have some residual sensitivity to the new channel. We found that the ATLAS search for $T \to t\,h$ in Ref. [6] is recastable and most sensitive to the signal for $a \to b\bar{b}$: it is based on a broad-band search with multiple signal regions using 0 or 1 lepton, many b tags, and cut-based hadronic top- and/or h_{bb} tags, which are loose enough to capture some of the new signal. Top partner searches tagging hadronic W and Z [9–11] use a 50%-efficient W-tagging working point [50] or a deep neutral network to tag boosted objects. They are potentially sensitive to $a \to gg$, however determining the tagging efficiency for a is very difficult with the available information.

Details and validation of the recasts are summarised in the Appendices.

In Fig. 2 we present the 95% C.L. limits in the m_T vs m_a plane for the three recast searches and for various combinations of BRs $a \to gg$ and $a \to b\bar{b}$. The grey areas are excluded by the excited top search [46], where a is tagged as a single QCD jet. They only cover very low masses, well below 50 GeV, with a slight dependence on the T mass, and the bound extends up to $m_T \approx 900$ GeV. The red regions in Fig. 2 are excluded by the 8 TeV RPV SUSY search [47]. The most sensitive signal region requires 7 jets with p_T larger than 80 GeV and at least two b-tagged jets, therefore the bound is the strongest for $BR(a \to bb) = 100\%$. Our bounds for $BR(a \to gg) = 100\%$ are significantly weaker than those in Ref. [20] for the same signal: while we recast the same search, we used the published results that have a larger estimate of the background compared to the note used by Ref. [20].[8] Finally, the blue regions in Fig. 2 are excluded by 13 TeV $T \to t\,h$ search [6]. We recast the "1-lepton regions", which target $T \to t\,h_{bb}$ by demanding at least

3 b-jets.[9] This search is, therefore, insensitive to the $a \to gg$ channel, however it gives strong bounds for $a \to b\bar{b}$ decays. It can be seen in Fig. 2 that the reach is maximised for $m_a \approx m_h$, for which the search is optimised. Yet, this T search can dominate the bound even for sub-dominant $b\bar{b}$ BR. We should note that our recast underestimates the bound on the $T \to t\,h$ channel mainly due to a marginally smaller signal efficiency and the fact that we do not combine different signal regions (see Appendix A.4 for more details).

Our results clearly show that for dominant $a \to gg$ decays, which is the norm in realistic models [36], the bound on m_T can be very weak: for $m_a \simeq 50$ GeV (which is not excluded by any direct searches [38]), $m_T \lesssim 400$ GeV is still allowed while for larger m_a the bound generically never passes ≈ 550 GeV. This represents a gap in the top partner coverage, which could be closed by dedicated searches tagging low-mass di-jet resonances. Note that this final state resembles a target signal with hadronic Z bosons, $tZ_{\text{had}}\bar{t}Z_{\text{had}}$. Another possible improvement would be to reduce the cuts on jet activity in the $\sqrt{s} = 13$ TeV search [48] to be able to cover the low mass region.

For dominant $T \to t\,a \to t\,b\bar{b}$, the bound for m_T exceeds 1 TeV for sufficiently heavy a. For light a (which implies collimated $b\bar{b}$ pairs), the T search looses sensitivity as search regions either demand a Higgs-tagged $b\bar{b}$-pair, or at least 4 sufficiently isolated b-jets. The coverage of this final state could also be improved by training an a-tagger algorithm in the low mass region.

3. Bounds for $BR(T \to t\,a) + BR(T \to t\,h) = 100\%$

The most general case where the pair-produced T can decay in all combinations of the four channels $b\,W$, $t\,Z$, $t\,h$ and $t\,a$ may seem daunting to analyse. However, the standard top partner searches are designed to cover final states when either one or both T decay in the focus channel, for instance $b\,W + X$ or $t\,Z + \bar{t}\,Z$, without contamination. If the signal regions have no sensitivity to the new channel $t\,a$, as is the case for leptonic Z or W decays for instance, then the presence of the new channel can be seen as an overall reduction of the effective cross section. For an "exclusive" search region which is sensitive to a particular combination of $T\bar{T}$ decays, the number of signal events is reduced by a factor of $(1 - BR_a)^2$. For an "inclusive" search region which targets final states $t\,Z + X$, $t\,h + X$ or $b\,W + X$ (with a specific decay of one top partner whilst not having strong requirements on the second), the number of events is reduced by a factor

$$\left.\frac{\sigma_{T,p}}{\sigma_{T,p}}\right|^{\text{eff}} = (1 - BR_a) + \frac{\epsilon_{\text{td}}}{2}BR_a BR_{\text{td}} + \mathcal{O}(\epsilon_{\text{td}}^2), \tag{3.1}$$

where BR_{td} is the branching ratio of T into the targeted decay channel in presence of BR_a, and ϵ_{td} is the signal efficiency to detect its decay products. These formulae allow for a simple rescaling of the bound.

As mentioned in the previous section, this simple estimate can fail in the case of $T \to t\,h$, as searches based on $h \to b\bar{b}$ can also be sensitive to $a \to b\bar{b}$, even for different masses as shown in Fig. 2. In this section, we therefore study the interplay of $t\,h$ and $t\,a$ decays in more detail. In particular, we consider a benchmark scenario in which T has two decay channels: $T \to t\,a$ and $T \to t\,h$. We fix $m_a = 50$ GeV, which corresponds to the weakest constrained mass value. For the decay of a, we consider two limiting scenarios: $BR(a \to gg) = 100\%$ and $BR(a \to b\bar{b}) = 100\%$. The

---

[7] Private communication.
[8] We checked that our recast is compatible with that of Ref. [20].

[9] The other "0-lepton" regions require large missing energy from invisible decays of the Z, thus they are not sensitive to the new channel.
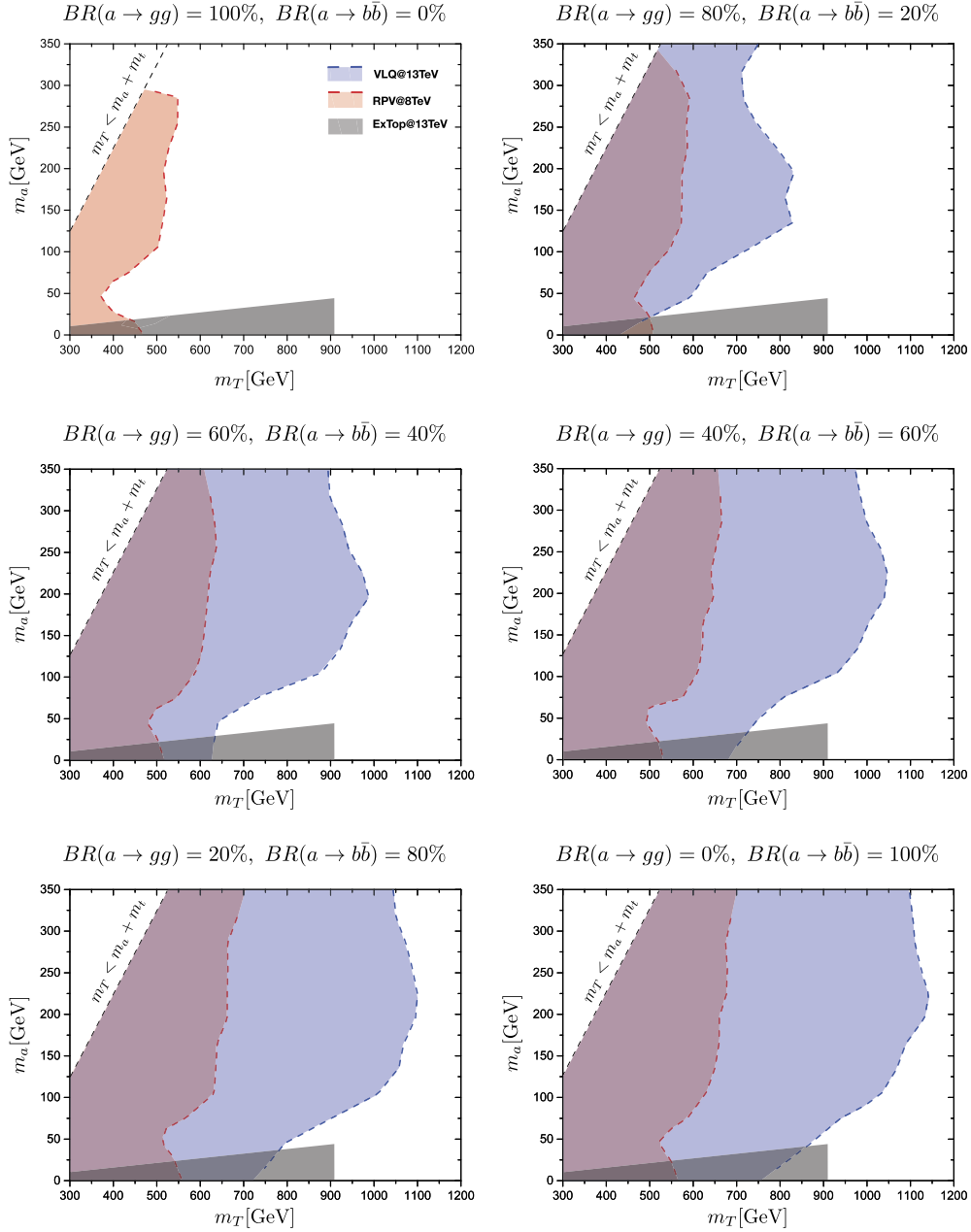
Fig. 2. Direct search limits on m_T vs m_a plane for different branching ratios of a to gg and $b\bar{b}$. In the region $m_T < m_a + m_t$, the $T \to ta$ decay is kinematically forbidden. The grey region at low m_a is excluded by CMS excited top search [46], as the boosted light a is tagged as a single jet. The red region is excluded by 8 TeV ATLAS multi-jets RPV SUSY search [47]. The blue region is excluded by 13 TeV ATLAS VLQ search [6]. Due to b-jet tagging requirements in the signal regions, limits to the model with a higher $BR(a \to b\bar{b})$ are more stringent.

results of the scan are shown in Fig. 3, where we demonstrate how the limit on m_T evolves for increasing BR($T \to t\ h$). In the case of $a \to gg$, low masses below 800 GeV are still allowed as long as BR$_h \lesssim 20\%$, while the mass bound remains strong otherwise and for $a \to b\bar{b}$. As a reference, we also show as a solid lines the naive estimate for the bound obtained by rescaling the number of signal events whilst assuming the search regions to be inclusive (top line, black) or exclusive (bottom line, grey). The reduction is translated into a bound on m_T under the assumption that the signal efficiency is approximately constant in the relevant m_T regime. As can be seen in Fig. 3 (left), the decrease of the bound with decrease of BR($T \to t\ h$) $= 1 -$ BR($T \to t\ a$) follows the shape expected for an exclusive search above BR($T \to t\ h$) ~ 0.6 while it follows the shape expected for an inclusive search region below,

indicating that the most constraining search regions differ in these two parameter regimes, and that the search has no explicit sensitivity to $T \to t\ a \to t\ gg$. Fig. 3 (right) clearly deviates from the naive scaling relation as the decay $T \to t\ a \to t\ b\bar{b}$ populates the signal regions.

4. Conclusions and outlook

Current LHC searches for vector-like top partners constrain a charge 2/3 top partner T to be heavier than $1.3 \div 1.4$ TeV, depending on the pattern of decays to the standard channels $t\ Z$, $t\ h$, or $b\ W$, exclusively. However, underlying models featuring partially composite tops always contain additional – potentially light – scalars, which provide common new decay modes for the top
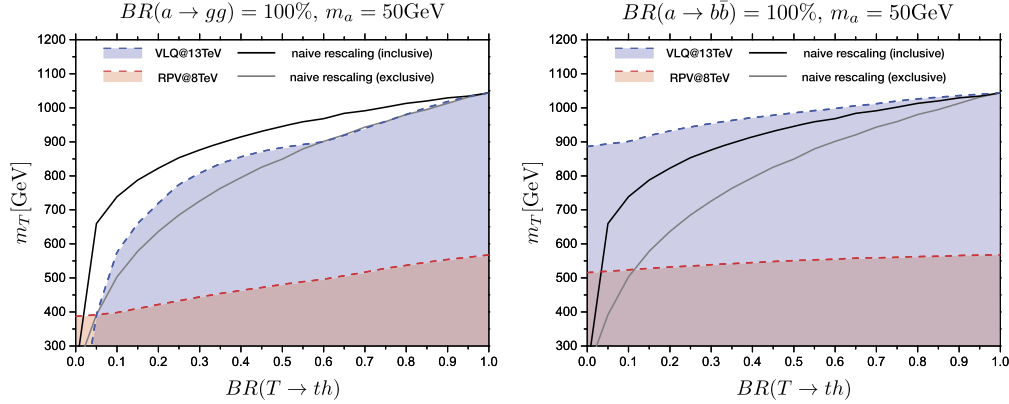
Fig. 3. Direct search limits on m_T as a function of BR($T \to th$). The red region is excluded by the $\sqrt{s} = 8$ TeV ATLAS multi-jets RPV SUSY search [47], while the blue region is excluded by the $\sqrt{s} = 13$ TeV ATLAS top partner search [6]. In both plots we fix $m_a = 50$ GeV. We also show bounds from naive rescaling. Black solid line and grey solid line correspond to inclusive search and exclusive search respectively.

partners. In particular, all models with an underlying confining gauge group and underlying fermions predict the existence of a light pseudo-Nambu-Goldstone boson, SM singlet, a that, if lighter than $2m_t$, decays dominantly to gg or $b\bar{b}$. This provides a theoretically well-justified motivation to focus on the exotic decays $T \to t\, a \to t\, gg$ and $T \to t\, a \to t\, b\bar{b}$.

In this letter, we studied top partner pair production via QCD interactions, followed by the exotic decays. We surveyed T pair production searches as well as other searches by ATLAS and CMS, and identified three searches that can be sensitive to the new final states: a broad-band $T \to t\, h$ search, a $\sqrt{s} = 8$ TeV RPV SUSY search, and the excited top-pair search. Besides being the most promising existing searches, they are easily recastable. The bounds we obtained show that the $T \to t\, a \to t\, gg$ channel is very weakly constrained, allowing for $m_T > 550$ GeV for any $m_a < 2m_t$ and going as low as $m_T \approx 390$ GeV for $m_a = 50$ GeV. The channel $T \to t\, a \to t\, b\bar{b}$ is better constrained due to the sensitivity of the broad-band $T \to t\, h$ search, although for light $m_a \lesssim 75$ GeV it looses sensitivity, allowing for m_T down to ≈ 900 GeV. We also provide estimates on the reduction of bounds if standard and exotic decays are both present, and study in detail the case of coexisting $T \to t\, h$ and $T \to t\, a$ decays in more detail. The latter is important as the search for $T \to t\, h$ also covers the exotic channel $T \to t\, a \to t\, b\bar{b}$, so a combined analysis is necessary.

Our analysis shows that, although exotic top partner decays can exhibit spectacular and well-constrained final states, there exist well-motivated channels that are very hard to constrain with current searches. In the case $T \to t\, a \to t\, gg$ we found that the bound on the T mass is strongly weakened, allowing values down to ≈ 400 GeV. Nevertheless, it is possible to increase the sensitivity to these final states by accordingly modifying the current searches. For example, the RPV SUSY search at $\sqrt{s} = 13$ TeV became insensitive to the $a \to gg$ channel because of a too-high cut on hadronic activity, which could be lowered in the future. Furthermore, $a \to jj$ decays resemble the hadronic decays of the W/Z and the Higgs in the SM, thus the sensitivity could also be improved by hadronic taggers, either cut-based or via BDT/machine learning techniques, which could identify di-jet resonances (boosted or resolved) with different masses. This problem is most severe for light a, with $m_a \lesssim m_W$, while heavier masses are covered, as shown by the reach of the $T \to t\, h \to t\, b\bar{b}$ broad-band search we recast. In the case of $T \to t\, a$, it is the over-specialised/trained cuts that "*pour the baby (signal) out with the bath water*". Future well-documented (recastable) broad-band searches or dedicated search regions targeting decay chains with $gg\,/\,b\bar{b}$ resonances with $m_{jj} \neq m_W, m_Z$ and/or $m_{bb} \neq m_h$ could close this gap.

Appendix A. Validation of recasts

All events are generated with MadGraph5 [51], then showered and hadronised with PYTHIA 8 [52]. DELPHES 3 is used for a fast detector simulation [53], and FastJet is used for jet clustering [54]. The $T\bar{T}$ production cross-section at $\sqrt{s} = 8$ TeV and 13 TeV LHC are calculated by Top++ [55]. In the following, we provide details of the recast and validation of the cut flows of the searches used in this article.

A.1. CMS 13 TeV excited top quark search

When the pseudo-scalar a is light and highly boosted, it resembles a single QCD jet. Thus, the effective final state of T pair production with a $T \to ta \to tgg$ or $tb\bar{b}$ decay is $t\bar{t}jj$, which is targeted by the search for excited top quark pair production [46]. This search, however, is not cut-flow based and a recast is not possible: we will therefore assume that the a decays are tagged as a single jet as long as the separation angle between the two jets is small enough.

To provide an estimate on the mass limit below which the pseudo-scalar a can be treated as single jet, we calculated the momentum a obtains from a T decaying at rest:

$$p = \frac{1}{2m_T}\sqrt{m_T^4 + m_t^4 + m_a^4 - 2m_T^2 m_t^2 - 2m_T^2 m_a^2 - 2m_t^2 m_a^2}$$
$$\approx \frac{1}{2m_T}\sqrt{m_T^4 + m_t^4 - 2m_T^2 m_t^2}\,. \tag{A.1}$$

If the decay direction of a is perpendicular to its propagation direction, then the angular distance between the decay products of a in the lab frame is:

$$\Delta\theta = 2\arctan\left(\frac{m_a}{p}\right) \approx \frac{4m_a m_T}{\sqrt{m_T^4 + m_t^4 - 2m_T^2 m_t^2}}\,. \tag{A.2}$$
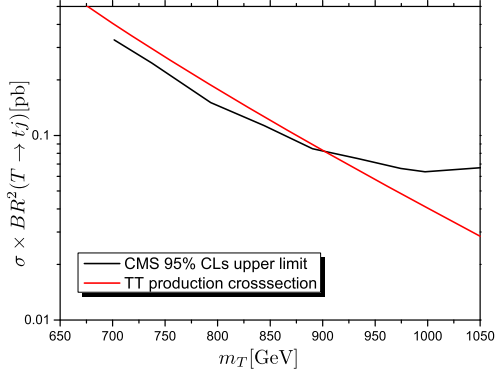
Fig. 4. Black line is the observed 95% CL_s upper limit for the T pair production cross-section times the square of BR$(T \to ta)$ as a function of m_T. The red line is the corresponding pair production cross-section at $\sqrt{s} = 13$ TeV LHC.

Table 1

Validation of our cut-flow reproduction of Ref. [47]. We provide event numbers after the full cut-flow for various benchmark models compared to the ATLAS ones in brackets.

Sample	SR		
	SR1(M_J^Σ)	$n_{jet} \geqslant 7$, $p_T \geqslant 120$ GeV, $n_b \geqslant 1$	$n_{jet} \geqslant 7$, $p_T \geqslant 80$ GeV, $n_b \geqslant 2$
$m_{\tilde{g}} = 600$ GeV, $m_{\tilde{\chi}_1^0} = 50$ GeV	85.8 (70)	200.9 (180)	–
$m_{\tilde{g}} = 1000$ GeV, $m_{\tilde{\chi}_1^0} = 600$ GeV	50.0 (55)	113.6 (101)	–
$m_{\tilde{g}} = 400$ GeV, $m_{\tilde{\chi}_1^0} = 50$ GeV	–	–	2135 (1900)
$m_{\tilde{g}} = 500$ GeV, BR(t)=0, BR(b)=1	–	–	2038 (1900)
$m_{\tilde{g}} = 500$ GeV, BR(t)=1, BR(b)=1	–	–	3159 (3600)
$m_{\tilde{g}} = 600$ GeV, BR(t)=1, BR(b)=1	–	–	2131 (2300)

Table 2

Validation of our cut-flow reproduction of Ref. [48]. We provide event numbers after each cut for two benchmark models compared to the ATLAS ones in brackets.

| Cut	Sample	
	$m_{\tilde{g}} = 1800$ GeV	$m_{\tilde{g}} = 1800$ GeV, $m_{\tilde{\chi}_1^0} = 1050$ GeV
Trigger	99.7 (99.7)	99.7 (99.7)
$n_{jet} \geqslant 4$	76.6 (74.1)	87.8 (88.4)
$|\Delta\eta_{12}| > 1.4$	67.9 (74.1)	79.6 (88.4)
$n_{jet} \geqslant 4$, $p_{T,j1} > 400$ GeV	67.9 (74)	79.4 (88.4)
$n_{jet} \geqslant 4$, $p_{T,j1} > 400$ GeV, $M_J^\Sigma > 1.0$ TeV	5.6 (7.38)	17.0 (25.4)
$n_{jet} \geqslant 4$, $p_{T,j1} > 400$ GeV, $N_{b-jet} > 0$	52.3 (52.9)	61.1 (69.6)
$n_{jet} \geqslant 4$, $p_{T,j1} > 400$ GeV, $N_{b-jet} > 0$, $M_J^\Sigma > 1.0$ TeV	4.3 (5.3)	13.1 (19.9)
$n_{jet} \geqslant 5$	30.5 (31.3)	48.1 (54.8)
$n_{jet} \geqslant 5$, $M_J^\Sigma > 0.8$ TeV	3.9 (5.4)	17.7 (26.9)
$n_{jet} \geqslant 5$, $N_{b-jet} > 0$	23.5 (22.6)	37.0 (43.5)
$n_{jet} \geqslant 5$, $N_{b-jet} > 0$, $M_J^\Sigma > 0.8$ TeV	3.0 (3.9)	13.6 (21.4)
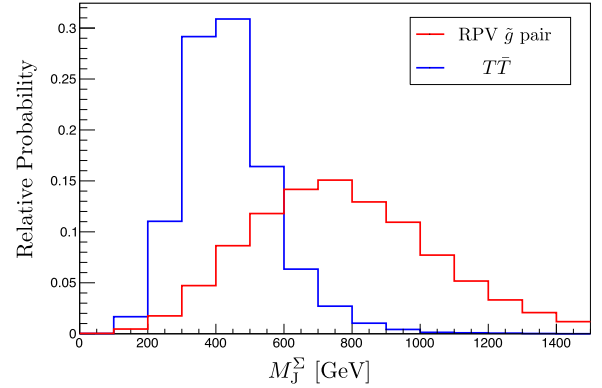
Fig. 5. Summed jet mass M_J^Σ distribution of a RPV gluino benchmark pair and of T pair. For the gluino signal we use the same benchmark used in Refs. [48] and [6]: $m_{\tilde{g}} = 1800$ GeV and $m_{\tilde{\chi}_1^0} = 1050$ GeV. For our signal we set $m_T = 1000$ GeV and $BR(T \to th) = 100\%$.

A.3. ATLAS 13 TeV RPV gluino pair search

Ref. [48] provides a detailed cut flow. Table 2 shows the event numbers after each cut as reported in Ref. [48] (in brackets) as well as event numbers we obtain in our recast, showing good agreement. For the signal considered in this article, however, the hard cut on summed jet mass M_J^Σ rejects most signal events. To illustrate this, we show the M_J^Σ distribution of an RPV gluino pair with $m_{\tilde{g}} = 1800$ GeV and $m_{\tilde{\chi}_1^0} = 1050$ GeV (a target benchmark of Ref. [48]) in comparison to a $T\bar{T}$ pair signal with $m_T = 1000$ GeV (a typical mass considered in this article) in Fig. 5.

A.4. ATLAS 13 TeV up-type vector-like quark search

A detailed cut flow table is not provided in Ref. [6]. We can thus only simulate and compare signal event numbers after applying the full set of cuts. We focus on the 1-lepton signal regions, which are most sensitive and for which signal efficiency and background

If $\Delta\theta$ is small enough, then most of the objects resulting from the a decay are clustered in a single jet. The jet clustering distance parameter R used in Ref. [46] is 0.4. Here, therefore, we assume that the boosted pseudo-scalar a with $\Delta\theta < 0.2$ is tagged as a single jet.

We further assume that the signal efficiency for the T and excited top quark are the same, provided their masses are equal. Thus, the cross section upper limit given in Ref. [46] can be used to directly constrain the exotic T decays. In Fig. 4 we show the 95% CL_s cross-section upper limit as function of the T mass compared to the production one: T masses lighter than 910 GeV are excluded, provided the branching ratio for $T \to ta$ is 100% and a is tagged as a single jet.

A.2. ATLAS 8 TeV RPV gluino pair search

A detailed cut flow table is not provided in Ref. [47]. We can thus only simulate and compare signal event numbers after applying the full set of cuts. Table 1 shows the signal event numbers we obtain in our recast as compared to those provided in Ref. [47] (in brackets).

Table 3
Validation of our cut-flow reproduction of Ref. [6]. We provide event numbers after the full cut-flow for various benchmark models compared to the ATLAS ones in brackets.

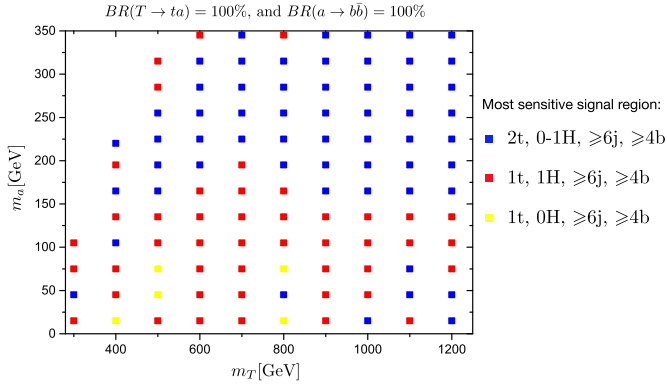| 1-lepton channel, $m_T = 1$ TeV, BR($T \to th$) = 100%				
$\geqslant$2t, 0-1H, $\geqslant$6j, 3b	1t, 0H, $\geqslant$6j, $\geqslant$4b	1t, 1H, $\geqslant$6j, $\geqslant$4b	$\geqslant$2t, 0-1H, $\geqslant$6j, $\geqslant$4b	$\geqslant$0t, $\geqslant$2H, $\geqslant$6j, $\geqslant$4b
18.3 (19.6)	15.6 (21.5)	15.3 (24.3)	17.8 (23.9)	9.7 (14.6)

Fig. 6. Most sensitive signal region for different m_T and m_a. Here we assume BR($T \to ta$) = 100% and BR($a \to b\bar{b}$) = 100%.

information is provided. Table 3 shows the signal event numbers we obtain in our recast as compared to those provided in Ref. [6] (in brackets).

The expected signal event number is sensitive to the multi b-jet tagging. The discrepancy between our result and Ref. [6] exceeds 20% in some cases, and our expected signal numbers are always smaller. Also, we do not combine bounds from different search regions and only report the largest bound from a single search region. Thus our recast underestimates the bound. For $T\bar{T}$ pair production with 100% branching ratio $T \to th$, we obtain a recast expected bound of $m_T > 1050$ GeV, while [6] reports an expected bound of $m_T > 1340$ GeV when combining all 0- and 1-lepton search regions.

Fig. 6 shows the most sensitive signal region for different m_T and m_a.

References

[1] D.B. Kaplan, H. Georgi, SU(2) x U(1) breaking by vacuum misalignment, Phys. Lett. B 136 (1984) 183–186.

[2] D.B. Kaplan, Flavor at SSC energies: a new mechanism for dynamically generated fermion masses, Nucl. Phys. B 365 (1991) 259–278.

[3] R. Contino, L. Da Rold, A. Pomarol, Light custodians in natural composite Higgs models, Phys. Rev. D 75 (2007) 055014, arXiv:hep-ph/0612048 [hep-ph].

[4] K. Agashe, R. Contino, A. Pomarol, The minimal composite Higgs model, Nucl. Phys. B 719 (2005) 165–187, arXiv:hep-ph/0412089 [hep-ph].

[5] A. De Simone, O. Matsedonskyi, R. Rattazzi, A. Wulzer, A first top partner Hunter's guide, J. High Energy Phys. 04 (2013) 004, arXiv:1211.5663 [hep-ph].

[6] ATLAS Collaboration, M. Aaboud, et al., Search for pair production of up-type vector-like quarks and for four-top-quark events in final states with multiple b-jets with the ATLAS detector, J. High Energy Phys. 07 (2018) 089, arXiv:1803.09678 [hep-ex].

[7] ATLAS Collaboration, M. Aaboud, et al., Search for pair- and single-production of vector-like quarks in final states with at least one Z boson decaying into a pair of electrons or muons in pp collision data collected with the ATLAS detector at $\sqrt{s} = 13$ TeV, Phys. Rev. D 98 (11) (2018) 112010, arXiv:1806.10555 [hep-ex].

[8] ATLAS Collaboration, M. Aaboud, et al., Search for pair production of vector-like top quarks in events with one lepton, jets, and missing transverse momentum in $\sqrt{s} = 13$ TeV pp collisions with the ATLAS detector, J. High Energy Phys. 08 (2017) 052, arXiv:1705.10751 [hep-ex].

[9] ATLAS Collaboration, M. Aaboud, et al., Search for pair production of heavy vector-like quarks decaying to high-p_T W bosons and b quarks in the lepton-plus-jets final state in pp collisions at $\sqrt{s} = 13$ TeV with the ATLAS detector, J. High Energy Phys. 10 (2017) 141, arXiv:1707.03347 [hep-ex].

[10] ATLAS Collaboration, M. Aaboud, et al., Search for pair production of heavy vector-like quarks decaying into hadronic final states in pp collisions at $\sqrt{s} = 13$ TeV with the ATLAS detector, Phys. Rev. D 98 (9) (2018) 092005, arXiv:1808.01771 [hep-ex].

[11] ATLAS Collaboration, M. Aaboud, et al., Search for pair production of heavy vector-like quarks decaying into high-p_T W bosons and top quarks in the lepton-plus-jets final state in pp collisions at $\sqrt{s} = 13$ TeV with the ATLAS detector, J. High Energy Phys. 08 (2018) 048, arXiv:1806.01762 [hep-ex].

[12] ATLAS Collaboration, M. Aaboud, et al., Combination of the searches for pair-produced vector-like partners of the third-generation quarks at $\sqrt{s} = 13$ TeV with the ATLAS detector, Phys. Rev. Lett. 121 (21) (2018) 211801, arXiv:1808.02343 [hep-ex].

[13] CMS Collaboration, A.M. Sirunyan, et al., Search for vector-like T and B quark pairs in final states with leptons at $\sqrt{s} = 13$ TeV, J. High Energy Phys. 08 (2018) 177, arXiv:1805.04758 [hep-ex].

[14] CMS Collaboration, A.M. Sirunyan, et al., Search for pair production of vector-like quarks in the bWbW channel from proton-proton collisions at $\sqrt{s} = 13$ TeV, Phys. Lett. B 779 (2018) 82–106, arXiv:1710.01539 [hep-ex].

[15] CMS Collaboration, A.M. Sirunyan, et al., Search for pair production of vector-like quarks in the fully hadronic final state, arXiv:1906.11903 [hep-ex].

[16] J. Serra, Beyond the minimal top partner decay, J. High Energy Phys. 09 (2015) 176, arXiv:1506.05110 [hep-ph].

[17] N. Bizot, G. Cacciapaglia, T. Flacke, Common exotic decays of top partners, J. High Energy Phys. 06 (2018) 065, arXiv:1803.00021 [hep-ph].

[18] H. Han, L. Huang, T. Ma, J. Shu, T.M.P. Tait, Y. Wu, Six top messages of new physics at the LHC, arXiv:1812.11286 [hep-ph].

[19] R. Benbrik, et al., Signatures of vector-like top partners decaying into new neutral scalar or pseudoscalar bosons, arXiv:1907.05929 [hep-ph].

[20] A. Anandakrishnan, J.H. Collins, M. Farina, E. Kuflik, M. Perelstein, Odd top partners at the LHC, Phys. Rev. D 93 (7) (2016) 075009, arXiv:1506.05130 [hep-ph].

[21] S. Kraml, U. Laa, L. Panizzi, H. Prager, Scalar versus fermionic top partner interpretations of $t\bar{t} + E_T^{miss}$ searches at the LHC, J. High Energy Phys. 11 (2016) 107, arXiv:1607.02050 [hep-ph].

[22] J.H. Kim, I.M. Lewis, Loop induced single top partner production and decay at the LHC, J. High Energy Phys. 05 (2018) 095, arXiv:1803.06351 [hep-ph].

[23] H. Alhazmi, J.H. Kim, K. Kong, I.M. Lewis, Shedding light on top partner at the LHC, J. High Energy Phys. 01 (2019) 139, arXiv:1808.03649 [hep-ph].

[24] J.A. Aguilar-Saavedra, D.E. López-Fogliani, C. Muñoz, Novel signatures for vector-like quarks, J. High Energy Phys. 06 (2017) 095, arXiv:1705.02526 [hep-ph].

[25] M. Chala, Direct bounds on heavy toplike quarks with standard and exotic decays, Phys. Rev. D 96 (1) (2017) 015028, arXiv:1705.03013 [hep-ph].

[26] R. Dermíšek, E. Lunghi, S. Shin, Hunting for vectorlike quarks, J. High Energy Phys. 04 (2019) 019, arXiv:1901.03709 [hep-ph].

[27] K.-P. Xie, G. Cacciapaglia, T. Flacke, Exotic decays of top partners with charge 5/3: bounds and opportunities, arXiv:1907.05894 [hep-ph].

[28] R. Contino, Y. Nomura, A. Pomarol, Higgs as a holographic pseudoGoldstone boson, Nucl. Phys. B 671 (2003) 148–174, arXiv:hep-ph/0306259 [hep-ph].

[29] R. Contino, A. Pomarol, Holography for fermions, J. High Energy Phys. 11 (2004) 058, arXiv:hep-th/0406257 [hep-th].

[30] G. Cacciapaglia, G. Marandella, J. Terning, Dimensions of supersymmetric operators from AdS/CFT, J. High Energy Phys. 06 (2009) 027, arXiv:0802.2946 [hep-th].

[31] M. Schmaltz, Physics beyond the standard model (theory): introducing the little Higgs, Nucl. Phys. B, Proc. Suppl. 117 (2003) 40–49, arXiv:hep-ph/0210415 [hep-ph], Nucl. Phys. B, Proc. Suppl. 40 (2002).

[32] I. Low, W. Skiba, D. Tucker-Smith, Little Higgses from an antisymmetric condensate, Phys. Rev. D 66 (2002) 072001, arXiv:hep-ph/0207243 [hep-ph].

[33] G. Ferretti, D. Karateev, Fermionic UV completions of composite Higgs models, J. High Energy Phys. 03 (2014) 077, arXiv:1312.5330 [hep-ph].

[34] J. Barnard, T. Gherghetta, T.S. Ray, UV descriptions of composite Higgs models without elementary scalars, J. High Energy Phys. 02 (2014) 002, arXiv:1311.6562 [hep-ph].

[35] G. Ferretti, Gauge theories of partial compositeness: scenarios for Run-II of the LHC, J. High Energy Phys. 06 (2016) 107, arXiv:1604.06467 [hep-ph].

[36] A. Belyaev, G. Cacciapaglia, H. Cai, G. Ferretti, T. Flacke, A. Parolini, H. Serodio, Di-boson signatures as standard candles for partial compositeness, J. High Energy Phys. 01 (2017) 094, arXiv:1610.06591 [hep-ph].

[37] T. DeGrand, M. Golterman, E.T. Neil, Y. Shamir, One-loop chiral perturbation theory with two fermion representations, Phys. Rev. D 94 (2) (2016) 025020, arXiv:1605.07738 [hep-ph].

[38] G. Cacciapaglia, G. Ferretti, T. Flacke, H. Serôdio, Light scalars in composite Higgs models, Front. Phys. 7 (2019) 22, arXiv:1902.06890 [hep-ph].

[39] G. Cacciapaglia, G. Ferretti, T. Flacke, H. Serodio, Revealing timid pseudo-scalars with taus at the LHC, Eur. Phys. J. C 78 (9) (2018) 724, arXiv:1710.11142 [hep-ph].

[40] M. Bauer, M. Neubert, A. Thamm, Collider probes of axion-like particles, J. High Energy Phys. 12 (2017) 044, arXiv:1708.00443 [hep-ph].

[41] M. Buchkremer, G. Cacciapaglia, A. Deandrea, L. Panizzi, Model independent framework for searches of top partners, Nucl. Phys. B 876 (2013) 376–417, arXiv:1305.4172 [hep-ph].

[42] D. Barducci, L. Panizzi, Vector-like quarks coupling discrimination at the LHC and future hadron colliders, J. High Energy Phys. 12 (2017) 057, arXiv:1710.02325 [hep-ph].

[43] LHCb Collaboration, R. Aaij, et al., Search for dark photons produced in 13 TeV pp collisions, Phys. Rev. Lett. 120 (6) (2018) 061801, arXiv:1710.02867 [hep-ex].

[44] CMS Collaboration, A.M. Sirunyan, et al., Search for resonances in the mass spectrum of muon pairs produced in association with b quark jets in proton-proton collisions at $\sqrt{s} = 8$ and 13 TeV, J. High Energy Phys. 11 (2018) 161, arXiv:1808.01890 [hep-ex].

[45] S. Moretti, D. O'Brien, L. Panizzi, H. Prager, Production of extra quarks at the Large Hadron Collider beyond the narrow width approximation, Phys. Rev. D 96 (7) (2017) 075035, arXiv:1603.09237 [hep-ph].

[46] CMS Collaboration, A.M. Sirunyan, et al., Search for pair production of excited top quarks in the lepton + jets final state, Phys. Lett. B 778 (2018) 349–370, arXiv:1711.10949 [hep-ex].

[47] ATLAS Collaboration, G. Aad, et al., Search for massive supersymmetric particles decaying to many jets using the ATLAS detector in pp collisions at $\sqrt{s} = 8$ TeV, Phys. Rev. D 91 (11) (2015) 112016, arXiv:1502.05686 [hep-ex]. Erratum: Phys. Rev. D 93 (3) (2016) 039901.

[48] ATLAS Collaboration, M. Aaboud, et al., Search for R-parity-violating supersymmetric particles in multi-jet final states produced in p-p collisions at $\sqrt{s} = 13$ TeV using the ATLAS detector at the LHC, Phys. Lett. B 785 (2018) 136–158, arXiv:1804.03568 [hep-ex].

[49] CMS Collaboration, A.M. Sirunyan, et al., Search for R-parity violating supersymmetry in pp collisions at $\sqrt{s} = 13$ TeV using b jets in a final state with a single lepton, many jets, and high sum of large-radius jet masses, Phys. Lett. B 783 (2018) 114–139, arXiv:1712.08920 [hep-ex].

[50] ATLAS Collaboration, M. Aaboud, et al., Identification of Boosted, Hadronically-Decaying W and Z Bosons in $\sqrt{s} = 13$ TeV Monte Carlo Simulations for ATLAS, Tech. Rep. ATL-PHYS-PUB-2015-033, CERN, Geneva, Aug 2015, https://cds.cern.ch/record/2041461.

[51] J. Alwall, R. Frederix, S. Frixione, V. Hirschi, F. Maltoni, O. Mattelaer, H.S. Shao, T. Stelzer, P. Torrielli, M. Zaro, The automated computation of tree-level and next-to-leading order differential cross sections, and their matching to parton shower simulations, J. High Energy Phys. 07 (2014) 079, arXiv:1405.0301 [hep-ph].

[52] T. Sjöstrand, S. Ask, J.R. Christiansen, R. Corke, N. Desai, P. Ilten, S. Mrenna, S. Prestel, C.O. Rasmussen, P.Z. Skands, An introduction to PYTHIA 8.2, Comput. Phys. Commun. 191 (2015) 159–177, arXiv:1410.3012 [hep-ph].

[53] DELPHES 3 Collaboration, J. de Favereau, C. Delaere, P. Demin, A. Giammanco, V. Lemaître, A. Mertens, M. Selvaggi, DELPHES 3, a modular framework for fast simulation of a generic collider experiment, J. High Energy Phys. 02 (2014) 057, arXiv:1307.6346 [hep-ex].

[54] M. Cacciari, G.P. Salam, G. Soyez, FastJet user manual, Eur. Phys. J. C 72 (2012) 1896, arXiv:1111.6097 [hep-ph].

[55] M. Czakon, A. Mitov, Top++: a program for the calculation of the top-pair cross-section at hadron colliders, Comput. Phys. Commun. 185 (2014) 2930, arXiv:1112.5675 [hep-ph].